EPJ Web of Conferences **303**, 05003 (2024) https://doi.org/10.1051/epjconf/202430305003
MENU 2023

Feasibility Studies for an Inclusive *R*-Measurement using ISR at BESIII

Thomas Lenz[1,*], *Achim* Denig[1], *Riccardo* Aliberti[1], and *Christoph Florian* Redmer[1]
on behalf of the BESIII Collaboration

[1]Institute for Nuclear Physics, Johannes Gutenberg University Mainz

Abstract. In this work a novel technique to measure the hadronic R value ($R = \sigma^0_{\mathrm{had}}/\sigma^0_{\mu\mu}$) inclusively is presented. The method employs the initial state radiation (ISR) technique and the study is carried out for the BESIII experiment at the tau-charm factory BEPC-II. Given the large Lorentz-boost of the hadronic system produced in an ISR process, the efficiency to detect at least one of the hadrons (once the ISR photon is reconstructed) is very high, thus relieving the reliance of the measurement on the theoretical model used in the simulations. A first inclusive determination of the R value in the low energy region can, therefore, be achieved, providing a crucial cross check to the current evaluations based on the sum of exclusive measurements.

1 Introduction

The magnetic moment of a charged lepton is given by $\vec{\mu}_l = g_l \frac{e}{2m_l}\vec{S}$, where g_l is the Landé factor and $l = e, \mu, \tau$. The anomaly of the magnetic moment is defined as the relative deviation of the Landé factor from the Dirac theory ($g_l^{\mathrm{Dirac}} = 2$ [1]):

$$a_l \equiv \frac{g_l - g_l^{\mathrm{Dirac}}}{g_l^{\mathrm{Dirac}}} = \frac{g_l - 2}{2} \,. \tag{1}$$

The anomalous magnetic moment of the muon has been measured very precisely in the last two decades by the Muon $g-2$ experiment at Brookhaven [2] and Fermilab [3, 4]. The current experimental world average is $a_\mu^{\mathrm{exp}} = (116\,592\,059 \pm 22) \times 10^{-11}$ achieving a precision of 189 ppb.

The Muon $g-2$ Theory Initiative published the Standard Model (SM) prediction [5–25] of $a_\mu^{\mathrm{SM}} = (116\,591\,810 \pm 43) \times 10^{-11}$ (369 ppb), which is in disagreement with the experiment by 5.1 σ (see Fig. 1). As shown in Tab. 1, the largest contributions to the uncertainty of the SM prediction stem from the hadronic processes: the hadronic vacuum polarization (HVP) and the hadronic light-by-light scattering (HLbL), which cannot be calculated perturbatively. Quantum Electrodynamics (QED) and electroweak (EW) contributions are, instead, known to better than 10 ppb.

Using a data-driven dispersive approach, the leading-order (LO) HVP contribution $a_\mu^{\mathrm{HVP,LO}}$ can be related to the total hadronic Born cross section σ^0_{had} in e^+e^- annihilation

*e-mail: lenz@uni-mainz.de

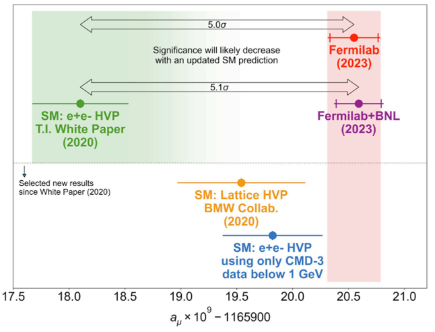

Figure 1: Comparison [26] of the experimental measurements [2–4] of a_μ and the theoretical evaluations of the Muon $g-2$ Theory Initiative [5–25] and different HVP evaluations using BMWc [27] or CMD-3 [28, 29] data.

Table 1: Contributions to the Standard Model prediction a_μ^{SM} of the Muon $g-2$ Theory Initiative [5–25].

	a_μ / 10^{-11}
QED	116 584 718.931 ± 0.104
EW	153.6 ± 1.0
HVP	6845 ± 40
HLbL	92 ± 18
Total	116 591 810 ± 43

using the Kernel function K [30, 31]:

$$a_\mu^{\mathrm{HVP,LO}} = \frac{1}{4\pi} \int_{m_\pi^2}^{\infty} \mathrm{d}s' \, K(s') \, \sigma^0_{\mathrm{had}}(s') \, , \tag{2}$$

where s' is the squared momentum transfer of the virtual photon. Given the $1/s'$ dependency of both the hadronic cross section and the Kernel function, the most relevant mass range contributing to a_μ is below 2 GeV.

Lattice QCD evaluations of $a_\mu^{\mathrm{HVP,LO}}$ have been performed by several collaborations. While there has been only one full evaluation with a competitive precision by BMWc [27] (0.8 %), other collaborations evaluated the contribution in a selected subset of the phase space [32, 33] and showed good agreement with BMWc. Using the results of BMWc in the evaluation of the SM prediction yields a value only deviating by 1.7 σ from the experimental world average.

Additionally to the Muon $g-2$ anomaly, the HVP is also an input to the running QED coupling constant at the Z pole, $\alpha_{\mathrm{QED}}(m_Z^2)$, which is used in EW precision fits [14, 15].

1.1 Hadronic *R* Value

The hadronic R value is defined as the total hadronic Born cross section normalized to the point-like Born cross section of the di-muon process:

$$R(s') \equiv \frac{\sigma^0(e^+e^- \to \gamma^* \to \mathrm{hadrons})(s')}{\sigma^0(e^+e^- \to \gamma^* \to \mu^+\mu^-)(s')} \, , \tag{3}$$

where s' is the squared momentum transfer of the virtual photon. It contains fundamental properties of QCD like the number of color charges and available quark flavors and resonances.

Due to the manifold of hadronic final states at higher energies, the measurement of R is divided into two regions: exclusive measurements below and inclusive measurements beyond the transition point around 2 GeV. At smaller energies, due to the low number of available channels, each channel is measured individually with high precision and the cross sections are combined afterwards.

The $\pi^+\pi^-$ channel, which mainly comes from decays of the $\rho(770)^0$ resonance, contributes over 70 % to the total value of $a_\mu^{\mathrm{HVP,LO}}$. The two most precise measurements to-date from KLOE [34–37] and BaBar [38, 39] deviate from each other by $2.8\,\sigma$. A recent measurement by CMD-3 [28, 29] increased the tension within the e^+e^- measurements even further. As shown in Fig. 1, using this result for the $\pi^+\pi^-$ channel in the evaluation of $a_\mu^{\mathrm{HVP,LO}}$ results in an even higher value than BMWc, closer towards the experimental value.

Inclusive measurements require a very good knowledge of the signal and background processes, since QED background needs to be subtracted and sizeable efficiency corrections need to be considered. Especially for the hadronic signal this is very challenging. The latest precise inclusive R measurement has been performed by BESIII [40] and uses a novel approach to validate the systematics of the hadronic event generators. A hybrid generator [41], consisting out of Phokhara [42], ConExc [43], and Luarlw [40, 44, 45] is used, which simulates 51 exclusive channels plus remaining unknown hadronic channels. For more details see Refs. [40, 46].

Given the tensions between KLOE, BaBar, and CMD-3 within the dispersive evaluation, the Lattice QCD evaluation by BMWc, and the experimental measurement of a_μ, a new, completely independent measurement and approach is highly desirable. This can be achieved by performing an inclusive R measurement below 2 GeV using the initial state radiation (ISR) technique.

2 BESIII Experiment

The Beijing Spectrometer III (BESIII) experiment is located at the Beijing Electron Positron Collider II (BEPC-II) at the Institute of High Energy Physics (IHEP) in Beijing, China [47].

The center-of-mass energy $\sqrt{s}$ is in the range of 2.0 GeV to 5.0 GeV. Its design luminosity of $1.0 \times 10^{33}\,\mathrm{cm}^{-2}\,\mathrm{s}^{-1}$ at the $\psi(3770)$ resonance was reached.

The detector has a solid angle coverage of $\frac{\Delta\Omega}{4\pi} = 0.93$ and consists of the following components: a multi-layer drift chamber (MDC), a time-of-flight system (TOF), and an electromagnetic calorimeter (EMC) within a homogenous magnetic field of 1 T. Additionally, it features a muon counter (MUC) system for muon identification.

3 Analysis Strategy

This feasibility study is based on $\mathcal{L}_{\mathrm{int}} = (3194.5 \pm 0.2_{\mathrm{stat.}} \pm 31.9_{\mathrm{sys.}})\,\mathrm{pb}^{-1}$ of data collected at a center-of-mass energy of $\sqrt{s} = (4178.0 \pm 0.1_{\mathrm{stat.}} \pm 0.8_{\mathrm{sys.}})\,\mathrm{MeV}$. The ISR photon is required to be detected at large scattering angles in the barrel part of the EMC ($|\cos\theta| < 0.8$, where θ is the polar angle to the symmetry axis of the detector). Since the relevant mass region for a_μ^{HVP}, containing the narrow resonances $\rho(770)^0$, $\omega(782)$, and $\phi(1020)$, is at small hadronic masses $\sqrt{s'}$, the energy of the ISR photon E_γ (in the e^+e^- rest frame), given by

$$E_\gamma = \frac{s - s'}{2\sqrt{s}}\,, \tag{4}$$

is very high (1.6 GeV to 2.1 GeV). The advantage of such high ISR photon energies is that the hadronic system is strongly Lorentz-boosted in the opposite direction and confined into a narrow cone. Charged hadrons are detected by the MDC, which covers the polar angle range of $|\cos\theta| < 0.93$. As can be seen in Fig. 2a, this ensures a very high efficiency to reconstruct at least one hadronic track. For channels containing charged particles (light blue line) it is around 98 % for the whole mass range. Neutral decays like $K^0_S \to \pi^0\pi^0$ or neutral channels like $\pi^0\gamma$ and $n\bar{n}$ lead to additional losses (dark blue line), which do not exceed 10 %. Thanks to such high efficiencies, only minor corrections, compared to established inclusive measurements, are needed and the reliance on the hadronic event generator is reduced.

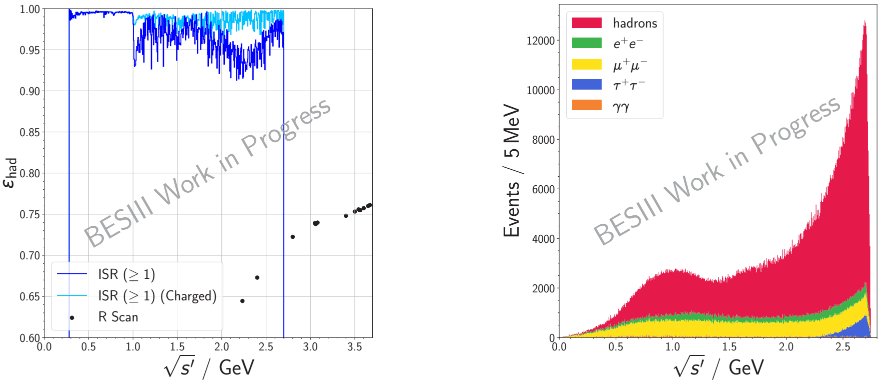

(a) Comparison of the hadronic efficiency ε_{had} as a function of hadronic mass $\sqrt{s'}$ of the ISR approach requiring at least one reconstructed charged track (for all events and truly charged events) and the BESIII R-scan [40].

(b) Hadronic mass $\sqrt{s'}$ spectrum for hadronic events (red) and QED background events (all other colors) after rejection criteria for QED processes applied.

Figure 2

The mass of the hadronic system $\sqrt{s'}$ is subsequently calculated from the recoil of the measured ISR photon, which is assumed to be the highest energetic reconstructed photon. The mass resolution is limited by the EMC and unable to resolve the narrow resonances. Thus, an unfolding [48] is required.

The Monte Carlo simulations used for the exclusive hadronic final states are PHOKHARA and CONEXC, while LUARLW is used for the remaining inclusive channels. The QED background contributions e^+e^-, $\gamma\gamma$, $\mu^+\mu^-$, and $\tau^+\tau^-$ are simulated by the high-precision generators BABAYAGA@NLO [49–53], PHOKHARA, and KKMC [54] respectively.

After selecting events with a high-energetic ISR photon (at least 1.2 GeV) at large angles and at least one charged track reconstructed in the MDC, the mass spectrum is dominated by QED, mainly (radiative) Bhabha scattering. Thus, using $\mathrm{d}E/\mathrm{d}x$ and TOF information, events containing tracks identified as electrons will be rejected. Additional cuts for e^+e^- and $\gamma\gamma$ final states are imposed to suppress those two-body kinematics. This does not completely eliminate all QED contributions, but leaves a smooth contribution which can be reliably subtracted. The resulting mass spectrum is dominated by hadronic contributions (Fig. 2b).

Although the majority of the remaining events are of hadronic nature, only a fraction of them are signal ISR events. Additional hadronic background contributions from high-energetic pseudoscalar meson decays, radiative charmonium decays, or $\bar{n}$ mimicking photons in the EMC arise especially at hadronic masses $\sqrt{s'}$ above 1.5 GeV. To suppress the largest contribution below 2 GeV, any combination of the ISR photon and another detected photon may not have an invariant mass close to the mass of the π^0 and η. After this requirement, the hadronic background is strongly reduced (Fig. 3).

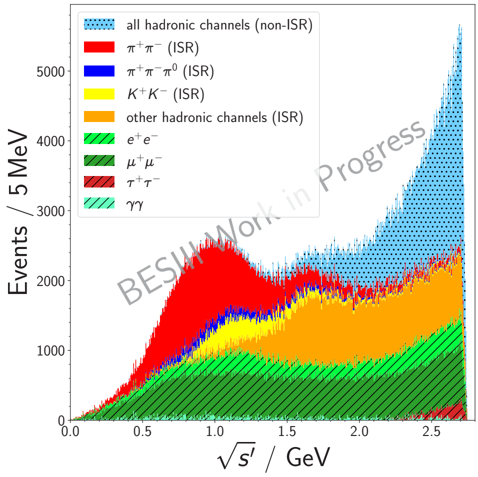

Figure 3: Hadronic mass $\sqrt{s'}$ spectrum after π^0 and η veto. The hatched area denotes QED background, while the dotted area stands for hadronic non-ISR contributions.

3.1 Alternative Approach: ISR Events with Pair Production

The ISR photon may produce an e^+e^- pair while interacting with the beam pipe or the MDC inner wall. Those secondary tracks are reconstructed using the method described in Ref. [55]. The reconstructed momenta of the leptons, and subsequently the four-momentum of the ISR photon, have a better resolution compared to the direct measurement using the EMC. This also propagates to an improved mass resolution of the hadronic system and yields a visible separation of the $\rho(770)^0$-$\omega(782)$ and $\phi(1020)$ peaks. The drawback of this alternative approach is, that, due to the additional interaction, the event yield is significantly reduced.

BESIII will have collected a data set of $20\,\text{fb}^{-1}$ at 3.773 GeV in the near future which will offer an excellent opportunity to use pair creation to measure R inclusively with higher precision.

4 Summary

This work presents a new independent approach to measure the R value inclusively below 2 GeV. Compared to established inclusive R measurements, the ISR technique utilizes the very high hadronic efficiency and thus minor efficiency corrections. This reduces the reliance on the accuracy of the hadronic Monte Carlo event generators, which is the main contribution to the systematic uncertainties in the existing measurements.

In order to achieve a competitive accuracy, the above mentioned issues regarding QED background subtraction, non-ISR hadronic events, and unfolding need to be worked out. The current studies have not identified limitations to achieve a precision of $\mathcal{O}(1\,\%)$. However, given the large discrepancies between the HVP evaluations using KLOE, BaBar, BMWc, or CMD-3 data, the precision aimed for will be sufficient to provide a new reference. The precision is expected to improve utilizing photon conversion events and a very high luminosity data set.

Additionally, if the neutral background, mainly from $\gamma\gamma$, is under control, this technique may also probe fully neutral (and potentially long-living) channels, as suggested in Ref. [56], which might not have been considered yet, without the need to detect a charged track.

References

[1] P.A.M. Dirac, Proc. Roy. Soc. Lond. A **117**, 610 (1928)
[2] G.W. Bennett et al. (Muon g-2), Phys. Rev. D **73**, 072003 (2006), `hep-ex/0602035`
[3] B. Abi et al. (Muon g-2), Phys. Rev. Lett. **126**, 141801 (2021), `2104.03281`
[4] D.P. Aguillard et al. (Muon g-2), Phys. Rev. Lett. **131**, 161802 (2023), `2308.06230`
[5] T. Aoyama et al., Phys. Rept. **887**, 1 (2020), `2006.04822`
[6] T. Aoyama, M. Hayakawa, T. Kinoshita, M. Nio, Phys. Rev. Lett. **109**, 111808 (2012), `1205.5370`
[7] T. Aoyama, T. Kinoshita, M. Nio, Atoms **7**, 28 (2019)
[8] A. Czarnecki, W.J. Marciano, A. Vainshtein, Phys. Rev. D **67**, 073006 (2003), [Erratum: Phys.Rev.D 73, 119901 (2006)], `hep-ph/0212229`
[9] C. Gnendiger, D. Stöckinger, H. Stöckinger-Kim, Phys. Rev. D **88**, 053005 (2013), `1306.5546`
[10] M. Davier, A. Höcker, B. Malaescu, Z. Zhang, Eur. Phys. J. C **77**, 827 (2017), `1706.09436`
[11] A. Keshavarzi, D. Nomura, T. Teubner, Phys. Rev. D **97**, 114025 (2018), `1802.02995`
[12] G. Colangelo, M. Hoferichter, P. Stoffer, JHEP **02**, 006 (2019), `1810.00007`
[13] M. Hoferichter, B.L. Hoid, B. Kubis, JHEP **08**, 137 (2019), `1907.01556`
[14] M. Davier, A. Höcker, B. Malaescu, Z. Zhang, Eur. Phys. J. C **80**, 241 (2020), [Erratum: Eur.Phys.J.C 80, 410 (2020)], `1908.00921`
[15] A. Keshavarzi, D. Nomura, T. Teubner, Phys. Rev. D **101**, 014029 (2020), `1911.00367`
[16] A. Kurz, T. Liu, P. Marquard, M. Steinhauser, Phys. Lett. B **734**, 144 (2014), `1403.6400`
[17] K. Melnikov, A. Vainshtein, Phys. Rev. D **70**, 113006 (2004), `hep-ph/0312226`
[18] P. Masjuan, P. Sanchez-Puertas, Phys. Rev. D **95**, 054026 (2017), `1701.05829`
[19] G. Colangelo, M. Hoferichter, M. Procura, P. Stoffer, JHEP **04**, 161 (2017), `1702.07347`
[20] M. Hoferichter, B.L. Hoid, B. Kubis, S. Leupold, S.P. Schneider, JHEP **10**, 141 (2018), `1808.04823`
[21] A. Gérardin, H.B. Meyer, A. Nyffeler, Phys. Rev. D **100**, 034520 (2019), `1903.09471`
[22] J. Bijnens, N. Hermansson-Truedsson, A. Rodríguez-Sánchez, Phys. Lett. B **798**, 134994 (2019), `1908.03331`
[23] G. Colangelo, F. Hagelstein, M. Hoferichter, L. Laub, P. Stoffer, JHEP **03**, 101 (2020), `1910.13432`
[24] T. Blum, N. Christ, M. Hayakawa, T. Izubuchi, L. Jin, C. Jung, C. Lehner, Phys. Rev. Lett. **124**, 132002 (2020), `1911.08123`
[25] G. Colangelo, M. Hoferichter, A. Nyffeler, M. Passera, P. Stoffer, Phys. Lett. B **735**, 90 (2014), `1403.7512`
[26] J. Mott, *Muon $g-2$ results* (2023), `https://indico.fnal.gov/event/60738/#3-muon-g-2-results`
[27] S. Borsanyi et al., Nature **593**, 51 (2021), `2002.12347`
[28] F.V. Ignatov et al. (CMD-3), Phys. Rev. D **109**, 112002 (2024), `2302.08834`
[29] F.V. Ignatov et al. (CMD-3), Phys. Rev. Lett. **132**, 231903 (2024), `2309.12910`
[30] S.J. Brodsky, E. De Rafael, Phys. Rev. **168**, 1620 (1968)
[31] B.E. Lautrup, E. De Rafael, Phys. Rev. **174**, 1835 (1968)
[32] T. Blum, P.A. Boyle, V. Gülpers, T. Izubuchi, L. Jin, C. Jung, A. Jüttner, C. Lehner, A. Portelli, J.T. Tsang (RBC, UKQCD), Phys. Rev. Lett. **121**, 022003 (2018),

1801.07224
[33] G. Colangelo, A.X. El-Khadra, M. Hoferichter, A. Keshavarzi, C. Lehner, P. Stoffer, T. Teubner, Phys. Lett. B **833**, 137313 (2022), 2205.12963
[34] F. Ambrosino et al. (KLOE), Phys. Lett. B **670**, 285 (2009), 0809.3950
[35] F. Ambrosino et al. (KLOE), Phys. Lett. B **700**, 102 (2011), 1006.5313
[36] D. Babusci et al. (KLOE), Phys. Lett. B **720**, 336 (2013), 1212.4524
[37] A. Anastasi et al. (KLOE-2), JHEP **03**, 173 (2018), 1711.03085
[38] B. Aubert et al. (BaBar), Phys. Rev. Lett. **103**, 231801 (2009), 0908.3589
[39] J.P. Lees et al. (BaBar), Phys. Rev. D **86**, 032013 (2012), 1205.2228
[40] M. Ablikim et al. (BESIII), Phys. Rev. Lett. **128**, 062004 (2022), 2112.11728
[41] R.G. Ping et al., Chin. Phys. C **40**, 113002 (2016), 1605.09208
[42] F. Campanario, H. Czyż, J. Gluza, T. Jeliński, G. Rodrigo, S. Tracz, D. Zhuridov, Phys. Rev. D **100**, 076004 (2019), 1903.10197
[43] R.G. Ping, Chin. Phys. C **38**, 083001 (2014), 1309.3932
[44] B. Andersson, *The Lund model*, Vol. 7 (Cambridge University Press, 2005), ISBN 978-0-521-01734-3, 978-0-521-42094-5, 978-0-511-88149-7
[45] B. Andersson, H.M. Hu (1999), hep-ph/9910285
[46] C.F. Redmer, in these proceedings (MENU2023) (2024)
[47] M. Ablikim et al. (BESIII), Nucl. Instrum. Meth. A **614**, 345 (2010), 0911.4960
[48] A. Höcker, V. Kartvelishvili, Nucl. Instrum. Meth. A **372**, 469 (1996), hep-ph/9509307
[49] G. Balossini, C.M. Carloni Calame, G. Montagna, O. Nicrosini, F. Piccinini, Nucl. Phys. B **758**, 227 (2006), hep-ph/0607181
[50] G. Balossini, C. Bignamini, C.M.C. Calame, G. Montagna, O. Nicrosini, F. Piccinini, Phys. Lett. B **663**, 209 (2008), 0801.3360
[51] C.M. Carloni Calame, G. Montagna, O. Nicrosini, F. Piccinini, Nucl. Phys. B Proc. Suppl. **131**, 48 (2004), hep-ph/0312014
[52] C.M. Carloni Calame, Phys. Lett. B **520**, 16 (2001), hep-ph/0103117
[53] C.M. Carloni Calame, C. Lunardini, G. Montagna, O. Nicrosini, F. Piccinini, Nucl. Phys. B **584**, 459 (2000), hep-ph/0003268
[54] S. Jadach, B.F.L. Ward, Z. Was, Comput. Phys. Commun. **130**, 260 (2000), hep-ph/9912214
[55] Z.R. Xu, K.L. He, Chin. Phys. C **36**, 742 (2012)
[56] G.R. Farrar (2022), 2206.13460